



## Overcoming barriers in long-term, continuous monitoring of soil CO<sub>2</sub> flux: A low-cost sensor system

Thi Thuc Nguyen<sup>1,2</sup>, Nadav Bekin<sup>1,3</sup>, Ariel Altman<sup>2</sup>, Martin Maier<sup>4</sup>, Nurit Agam<sup>3</sup>, Elad

5 Levintal<sup>2,\*</sup>

<sup>1</sup>Kreitman School of Advanced Graduate Studies, Ben-Gurion University of the Negev, Be'er Sheva, 840071, Israel

<sup>2</sup>Zuckerberg Institute for Water Research, The Jacob Blaustein Institutes for Desert Research, Ben-Gurion University of the Negev, Sde Boker campus, 84990, Israel

10 <sup>3</sup>French Associates Institute for Agriculture and Biotechnology of Drylands, The Jacob Blaustein Institutes for Desert Research, Ben-Gurion University of the Negev, Sde Boker campus, 84990, Israel

<sup>4</sup>Department of Crop Sciences, Chair of Soil Physics, University of Göttingen, Grisebachstraße 6, 37077, Göttingen, Germany

\*Correspondence to: Elad Levintal ([levintal@bgu.ac.il](mailto:levintal@bgu.ac.il))

15



### Abbreviations

- 20 CM, chamber method.
- $C_{ref}$ , reference CO<sub>2</sub> concentration measured by Vaisala CO<sub>2</sub> sensor and LI-COR gas analyzer.
- $C_{SCD30}$ , CO<sub>2</sub> concentration measured by low-cost SCD30 CO<sub>2</sub> sensors.
- $F_{CM}$ , soil CO<sub>2</sub> flux measured by chamber method.
- $F_{GM}$ , soil CO<sub>2</sub> flux calculated by gradient method.
- 25  $F_s$ , soil CO<sub>2</sub> flux.
- GM, gradient method.
- LC-SS, low-cost sensor system.
- NDIR, non-dispersive infrared.
- SD, secure digital.
- 30 SWC, soil water content.



**Abstract.** Soil CO<sub>2</sub> flux ( $F_s$ ) is a carbon cycling metric crucial for assessing ecosystem carbon budgets and global warming. However, global  $F_s$  datasets often suffer from low temporal-spatial resolution, as well as from spatial bias.  $F_s$  observations are severely deficient in tundra and dryland ecosystems due to financial and logistical constraints of current methods for  $F_s$  quantification. In this study, we introduce a  
35 novel, low-cost sensor system (LC-SS) for long-term, continuous monitoring of soil CO<sub>2</sub> concentration and flux. The LC-SS, built from affordable, open-source hardware and software, offers a cost-effective solution (~USD700), accessible to low-budget users, and opens the scope for research with a large number of sensor system replications. The LC-SS was tested over ~6 months in arid soil conditions, where fluxes are small, and accuracy is critical. CO<sub>2</sub> concentration and soil temperature were measured  
40 at 10-min intervals at depths of 5 and 10 cm. The LC-SS demonstrated high stability and minimal maintenance requirements during the tested period. Both diurnal and seasonal soil CO<sub>2</sub> concentration variabilities were observed, highlighting the system's capability of continuous, long-term, in-situ monitoring of soil CO<sub>2</sub> concentration. In addition,  $F_s$  was calculated using the measured CO<sub>2</sub> concentration via the gradient method and validated with  $F_s$  measured by the flux chamber method using  
45 the well-accepted LI-COR gas analyzer system. Gradient method  $F_s$  was in good agreement with flux chamber  $F_s$ , highlighting the potential for alternative or concurrent use of the LC-SS with current methods for  $F_s$  estimation. Leveraging the accuracy and cost-effectiveness of the LC-SS (below 10 % of automated gas analyzer system cost), strategic implementation of LC-SSs could be a promising means to effectively increase the number of measurements, spatially and temporally, ultimately aiding in  
50 bridging the gap between global  $F_s$  uncertainties and current measurement limitations.



## 1. Introduction

Soil is the largest terrestrial carbon pool (Lal, 2005). Soil carbon can be subdivided into two general pools: organic and inorganic, with the global storage of each pool at approximately 1,530 and 940 PgC, respectively (Monger et al., 2015). Both organic and inorganic soil carbon exchange with the atmosphere through soil CO<sub>2</sub> flux ( $F_s$ ).  $F_s$  is one of the largest carbon fluxes in the Earth system (Bond-Lamberty, 2018; Friedlingstein et al., 2022). Compared with human-caused increases in atmospheric CO<sub>2</sub>, annual CO<sub>2</sub> efflux from the soil into the atmosphere is much larger (Oertel et al., 2016). Therefore,  $F_s$  is considered a crucial carbon cycling metric, contributing to determining an ecosystem's carbon budget and assessing the current global warming scenarios (Bond-Lamberty et al., 2024; Xiao et al., 2012).

For decades, there has been a lack of  $F_s$  monitoring in different parts of the globe. Various initiatives have been undertaken to integrate dispersed  $F_s$  observations worldwide into publicly accessible datasets (Bond-Lamberty et al., 2020; Bond-Lamberty and Thomson, 2010; Jian et al., 2021). However, global  $F_s$  datasets often exhibit low temporal-spatial resolution and spatial bias (Stell et al., 2021; Warner et al., 2019). These limitations constrain our understanding of the mechanisms governing soil carbon dynamics and bias regional-to-global  $F_s$  estimation. The largest uncertainties in  $F_s$  estimates are found in tundra and dryland ecosystems primarily situated at the two poles, across Africa, Central Asia, South America, and Australia (Stell et al., 2021; Warner et al., 2019; Xu and Shang, 2016). These gaps can be primarily attributed to logistical constraints in manual data collection and the high costs of commercial measuring devices (Bouma, 2017; Forbes et al., 2023; Xu and Shang, 2016). Addressing logistical and financial constraints is crucial because critical questions concerning carbon dynamics can only be answered through extensive  $F_s$  quantification (Kim et al., 2022).

Field methods commonly used worldwide to quantify  $F_s$  are the eddy covariance method (Baldocchi et al., 1988; Massman and Lee, 2002), the flux chamber method (CM) (Davidson et al., 2002; Lundegårdh, 1927), and the gradient method (GM) (De Jong and Schappert, 1972; Hirano et al., 2003; Tang et al., 2003). These methods substantially differ in principles, thus deviating in cost and  $F_s$  estimation. The eddy covariance method provides  $F_s$  from a relatively large surface area (Gu et al., 2012), whereas the CM and GM yield single-point  $F_s$  (Bekin & Agam, 2023; Maier and Schack-Kirchner, 2014). The CM allows  $F_s$  to be measured directly from the soil surface, while the GM measures subsurface soil CO<sub>2</sub> concentration and estimates  $F_s$  using Fick's law (Maier and Schack-Kirchner, 2014).

Despite the increasing popularity of the eddy covariance and CM, the GM remains a useful, widely used method (Chamizo et al., 2022; Hirano et al., 2003; Tang et al., 2003; Vargas et al., 2010). In comparison to the other two methods, the GM offers several advantages. First, it mitigates issues associated with eddy covariance, such as turbulence insufficiency, and with CM, such as the microclimate alterations from chamber deployment (Bekin and Agam, 2023; Maier and Schack-Kirchner, 2014). Moreover, GM offers additional insights into the depth profile of gas production, consumption, and exchange in the soil (Maier and Schack-Kirchner, 2014). The most significant advantage of the GM is its lower purchase and installation costs (1- 2 orders of magnitude less than the CM or eddy covariance method for continuous  $F_s$  monitoring).



The development of small, low-cost, low-power, environmental sensors, microcontrollers, and microcomputers has significantly advanced (Chan et al., 2021; Levintal, Suvočarev, et al., 2021). This advancement has led to the extended adoption of low-cost environmental sensing systems in the scientific community (e.g., Helm et al., 2021). Attempts to monitor soil CO<sub>2</sub> concentration using low-cost CO<sub>2</sub> sensors have been made (Blackstock et al., 2019; Hassan et al., 2023; Heger et al., 2020; Osterholt et al., 2022). Others monitored CO<sub>2</sub> fluxes, such as stem, terrestrial, and aquatic fluxes, by implementing the CM using low-cost CO<sub>2</sub> sensors and data loggers (Bastviken et al., 2015; Gagnon et al., 2016; Brändle & Kunert, 2019; Carbone et al., 2019; Forbes et al., 2023; Helm et al., 2021). Implementing the GM using soil CO<sub>2</sub> concentrations measured by underground CO<sub>2</sub> sensors was also reported (Osterholt et al., 2022). However, these studies primarily focused on comparing the precision and accuracy of the low-cost systems with high-end reference systems, typically conducting short-term in-situ examinations lasting from days to weeks, which limits insights into their stability and practicality for long-term use.

To narrow the gap between the uncertainties in the regional-to-global  $F_s$  estimations and the capabilities of current measurement methods, in this study, we introduce an open-source, low-cost sensor system (LC-SS) for continuous, long-term monitoring of soil CO<sub>2</sub> concentrations and  $F_s$ . The LC-SS was field-tested over ~6 months in arid soil conditions to examine its stability and accuracy compared to a commercial automated flux chamber. Detailed, step-by-step, do-it-yourself guides describing the design, assembly, and installation are provided to assist non-engineer end-users with easy replication and customization.

## 2. Materials and methods

### 2.1. Hardware

The LC-SS consists of two units: the control unit and the sensing unit (**Fig. 1a** & **Fig. S1**). The control unit includes a microcontroller (Feather M0 Adalogger, Adafruit, USA) accompanied by Secure Digital (SD) card, a latching relay for power control (Latching mini FeatherWing, Adafruit, USA), a clock for accurate time readings (DS3231 RTC, Adafruit, USA), a screen to display real-time results (0.96" 128x64 OLED Graphic Display, Adafruit, USA), and a multiplexer allowing communication to the sensing unit (Gravity 1-to-8 I2C Multiplexer, DFRobot, China). For power, the microcontroller uses a 3.7 V lithium-ion polymer battery (3.7 V 6000 mAh, Adafruit, USA) charged by solar energy via a solar charger (bq24074, Adafruit, USA), and a 6 W 6 V solar panel (Adafruit, USA). The sensing unit includes seven sensors: six CO<sub>2</sub> sensors (SCD30, Sensirion, Switzerland, 0-10,000 ppm, accuracy between 400 to 10,000 ppm:  $\pm 30$  ppm + 3 % of full range), and an atmospheric microclimate sensor (pressure, relative humidity, and temperature, MS8607, DFRobot, China). The SCD30 CO<sub>2</sub> sensor also measures temperature and relative humidity (accuracy:  $\pm 0.4$  °C and  $\pm 3$  %, respectively).

The LC-SS used in this study featured two waterproof designs of CO<sub>2</sub> sensors (**Fig. 1b**): a 50 ml Falcon tube design and a thin coating design. The 50 ml Falcon tube design is an easy-made and long-lasting option, while the thin coating design is suitable for near-surface deployment, effectively reducing errors associated with measurement depths. Both designs included a hydrophobic membrane to keep water from penetrating the sensor while allowing gas exchange with the surrounding soil. Providing two designs



130

offers end users the flexibility to adopt the option that best fits their needs and accessibility. The detailed do-it-yourself guide of the LC-SS assembly and sensor waterproof designs can be found on our GitHub page ([https://github.com/OpenDigiEnvLab/soil-CO<sub>2</sub>-sensor-system](https://github.com/OpenDigiEnvLab/soil-CO2-sensor-system)). The hardware details are summarized in **Table 1**.

**Table 1.** Summary of hardware components with examples for potential suppliers (components can be purchased from other suppliers).

Component	Quantity	Cost/item (USD)	Sources	Comments
Feather M0 Adalogger	1	19.95	Adafruit ( <a href="https://www.adafruit.com/product/2796">https://www.adafruit.com/product/2796</a> )	A low-cost, low-power data logger
RTC DS3231 with CR1220 battery	1	17.5	Adafruit ( <a href="https://www.adafruit.com/product/3013">https://www.adafruit.com/product/3013</a> )	Provides accurate time for the data logger; CR1220 battery should be purchased separately
Gravity 1-to-8 I2C Multiplexer	1	6.9	DFRobot ( <a href="https://www.dfrobot.com/product-1780.html">https://www.dfrobot.com/product-1780.html</a> )	Enables the connection of multiple CO <sub>2</sub> sensors to one data logger
0.96" 128x64 OLED Graphic Display	1	17.5	Adafruit ( <a href="https://www.adafruit.com/product/326">https://www.adafruit.com/product/326</a> )	For real-time display of measurement results
Latching relay FeatherWing	1	7.95	Adafruit ( <a href="https://www.adafruit.com/product/2923">https://www.adafruit.com/product/2923</a> )	For power control: programmed to turn on and turn off the system to optimize power consumption
P2886A feather header kit	1	0.95	Adafruit ( <a href="https://www.adafruit.com/product/2886">https://www.adafruit.com/product/2886</a> )	To connect Feather M0 Adalogger with Latching relay FeatherWing
Lithium Ion Battery Pack-3.7 V 6600 mAh	1	24.5	Adafruit ( <a href="https://www.adafruit.com/product/353">https://www.adafruit.com/product/353</a> )	To provide power for the control and sensor unit
Adafruit Universal USB / DC / Solar Lithium Ion/Polymer charger - bq24074	1	14.95	Adafruit ( <a href="https://www.adafruit.com/product/4755">https://www.adafruit.com/product/4755</a> )	To charge the battery using the solar energy from solar panel
Medium 6 V-2 W Solar panel	1	29	Adafruit ( <a href="https://www.adafruit.com/product/200">https://www.adafruit.com/product/200</a> )	
SD/MicroSD memory card (8GB SDHC)		9.95	Adafruit ( <a href="https://www.adafruit.com/product/1294">https://www.adafruit.com/product/1294</a> )	
SCD30 CO <sub>2</sub> sensors	6	61.79	Digikey ( <a href="https://www.digikey.com/en/products/detail/sensirion-ag/SCD30/8445334">https://www.digikey.com/en/products/detail/sensirion-ag/SCD30/8445334</a> )	4 sensors with thin coating and 2 sensors with 50ml falcon tube
STEMMA QT MS8607 humidity-temperature-pressure sensor	1	14.95	Adafruit ( <a href="https://www.adafruit.com/product/4716">https://www.adafruit.com/product/4716</a> )	To measure atmospheric humidity, temperature, and pressure
Weather-proof container	1	10	Local suppliers	For the control unit
3D-printed frame	4	2	Printed locally	For thin coating of 4 sensors
Epoxy	500 grams	5	Local suppliers	For thin coating of 4 sensors
Plasti Dip	50 ml	5	Local suppliers	For thin coating of 4 sensors



Cables, wires, and general equipment: + 7 × 4-wire cable 3 m (6 for SCD30 sensors and 1 for MS8607 sensor) + Wires in colors white, green, red, black + 8 × 4-pin cables with Female Dupont connectors + 3 × JST PH 2-pin cable-male connector + 1 × 4-pin PH2.0 cable-male connector + 2 lever wire connectors + On/off switch + Shrinking sleeves of different sizes + Superglue		~50	Local suppliers
---	--	-----	-----------------

135 The hardware is controlled using open-source Arduino code written in C++ ([www.arduino.cc](http://www.arduino.cc)). The complete code uploaded to the LC-SS can be downloaded from our GitHub page. During every measurement cycle, all sensors are activated, and measurement readings are logged onto the SD card with a timestamp and displayed on the user screen. The default measurement interval is 10 minutes and can be easily customized if required.

## 2.2. Field installation

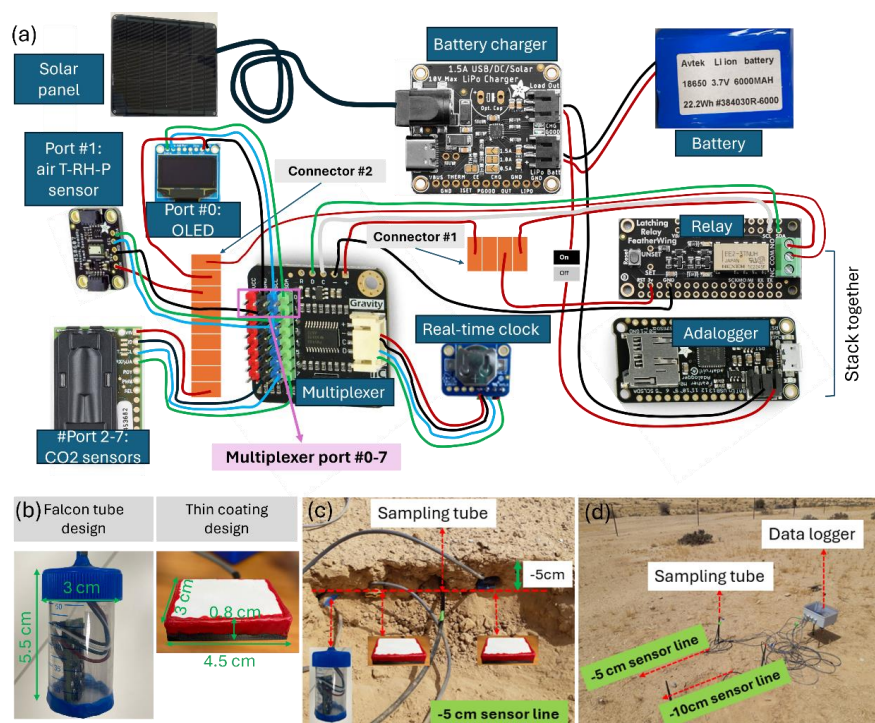
140 The LC-SS was installed at the Wadi Mashash Experimental farm located in the Northern Negev desert of Israel (31°04'14'' N, 34°51'62'' E; 360 meters above sea level). The local climate is arid, with an average annual precipitation of 116 mm, primarily occurring between October and April. The daily average maximum and minimum temperatures in January (winter) are 15.9 °C and 8.0 °C, and in August (summer) are 33.3 °C and 20.7 °C, respectively. Soil is characterized as sandy-loam loess soil (72.5 % sand, 15 % silt, and 12.5 % clay). Soil organic matter content between 0-5 and 5-10 cm is 2.96 and 2.62 %  
 145 %, respectively. CaCO<sub>3</sub> content between 0-5 and 5-10 cm is 50 and 47 %, respectively.

The LC-SS was installed from 24/05/2023 to 14/11/2023, providing continuous measurements for 175 successive days, spanning both summer and winter. Three CO<sub>2</sub> sensors were installed at each depth (5 and 10 cm) to allow comparison and statistical calibration, as detailed in section 2.3. At each depth, two sensors with a thin coating design (labeled as sensor#1\_5cm, sensor#2\_5cm and sensor#1\_10cm, sensor#2\_10cm) and one sensor with the 50 ml Falcon tube design (labeled as sensor#3\_5cm and sensor#3\_10cm) were deployed (**Fig. 1c**). To enable manual gas sampling during field calibration campaigns, a 60-cm Polyurethane tube (outer diameter × inner diameter = 6×4 mm) was inserted at each depth. One end of the tube was aligned with the CO<sub>2</sub> sensors, while the other end extended above the soil surface and was sealed with a valve (**Fig. 1d**). Additional measurements included soil water content (SWC) using time-domain reflectometers (TDR-315, Acclima, Inc., USA) installed at 3 and 10 cm  
 155 depths. Air temperature, atmospheric pressure, and precipitation data were taken from a meteorological



station located at the same field where the LC-SS was installed (<https://ims.gov.il>; Zomet Hanegev station).

160  $F_s$  measured using the CM ( $F_{CM}$ ) was measured at 1-hour intervals using a non-dispersive infrared (NDIR) gas analyzer (LI-8100A, LI-COR, USA) connected to four automated non-steady-state chambers (104C, LI-COR, USA).  $F_{CM}$  was determined as the average readings obtained from the four chambers. The  $F_{CM}$  measurements were conducted for the periods 24/05-18/06, 17-23/08, and 5/9-17/10/2023.



165 **Figure 1: The design of the low-cost sensor system (LC-SS) (a), two waterproof designs for the SCD30 CO<sub>2</sub> sensors (b), field installation of the CO<sub>2</sub> sensor line at 5 cm (c), and the site after installation (d).**

### 2.3. Two-step calibration of the CO<sub>2</sub> sensors

170 Calculating  $F_s$  based on the GM ( $F_{GM}$ ) (section 2.4) requires accurate soil CO<sub>2</sub> concentrations. Therefore, we developed a two-step calibration process for the underground CO<sub>2</sub> sensors: a field calibration and a statistical calibration.

For the field calibration, CO<sub>2</sub> concentrations from the low-cost SCD30 CO<sub>2</sub> sensors ( $C_{SCD30}$ ) were calibrated against reference CO<sub>2</sub> concentrations ( $C_{ref}$ ).  $C_{ref}$  were obtained by measuring the CO<sub>2</sub> concentrations sampled from the sampling tube either by a high-end CO<sub>2</sub> sensor (GMP252, Vaisala Inc., Finland) or by LI-COR gas analyzer (LI-8100A, LI-COR, USA) with three replicates from each depth (depending on field availability).  $C_{ref}$  by the Vaisala CO<sub>2</sub> sensor was measured every 5 hours between





6:00 and 16:00 on two days, 12/06 and 17/07/2023.  $C_{ref}$  by the NDIR gas analyzer was measured every 3 hours from 12:00 to 21:00 on 10/9/2023 and from 00:00 to 12:00 on 11/09/2023. In total, the calibration was determined with 21 and 17 measurement points for each sensor at 5 and 10 cm, respectively, over  
 180 the range of concentrations from ~300 to ~650 ppm.

The statistical calibration consisted of two sequential algorithms. The first algorithm (Fig. 2a) addressed abrupt anomalies or jumps of each sensor reading by flagging data points where the difference between measured and smoothed data exceeded 10 % of the measured data point. The smoothed data was executed using the LOESS smoothing algorithm (Jacoby, 2000), which fits multiple locally weighted least squares regressions to estimate a smooth curve through a scatterplot of data points. The second algorithm (Fig. 2b) focused on detecting and correcting gradual drift, utilizing user-defined thresholds to determine when the difference between one sensor and the other two sensors becomes significant enough to require correction. Thresholds of 5 % and 10 % relative to the average for sensors at 5 and 10 cm, respectively, were defined. All calibration algorithms were applied post-data acquisition, ensuring accurate  $CO_2$   
 185 concentrations essential for calculating  $F_{GM}$ .  
 190

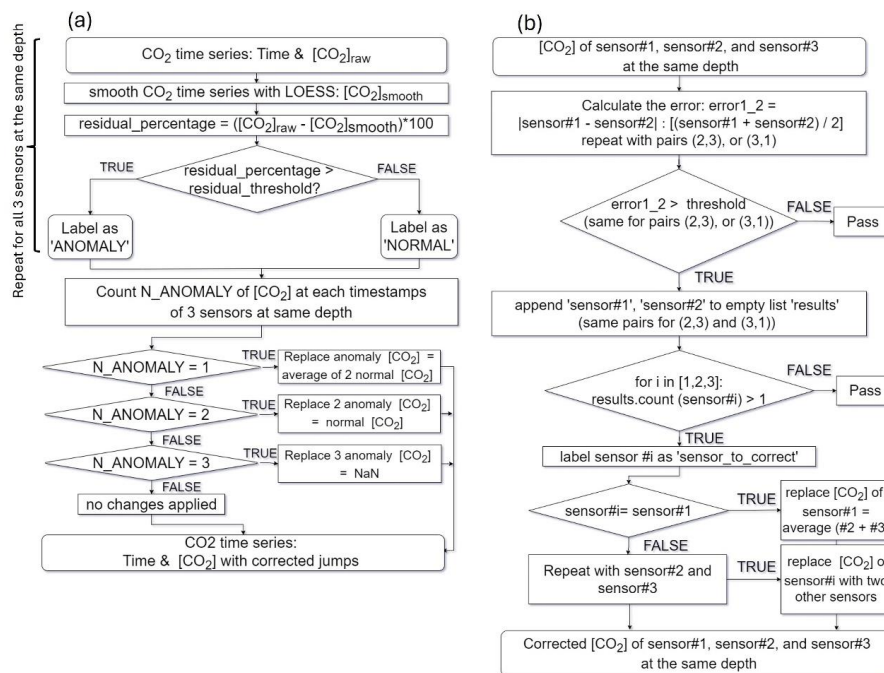


**Figure 2: Flowchart of the two statistical calibration algorithms. The algorithm to correct jumps (a) and the algorithm to correct gradual drift (b).**

#### 2.4. Calculating the $F_{GM}$ using the LC-SS data



195 To calculate  $F_{GM}$ , CO<sub>2</sub> concentrations were first corrected for temperature and pressure (**Eq. S1**) and then converted to mole density (**Eq. S2**). The GM is based on Fick's first law, where  $F_{GM}$  from depth  $z$  to the soil surface is calculated as (De Jong and Schappert, 1972):

$$F_{GM} = -D_s \frac{C_z - C_0}{z} \quad [1]$$

where  $F_{GM}$  [ $\mu\text{mol m}^{-2} \text{s}^{-1}$ ] is assumed to be equal to  $F_s$  from the soil surface (a positive  $F_{GM}$  indicates CO<sub>2</sub> efflux and a negative  $F_{GM}$  indicates CO<sub>2</sub> influx),  $D_s$  [ $\text{m}^2 \text{s}^{-1}$ ] is the CO<sub>2</sub> diffusion coefficient between  
 200 depth  $z$  [m] (negative) and the soil surface (0 m),  $C_z$  [ $\mu\text{mol m}^{-3}$ ] is the CO<sub>2</sub> mole density at depth  $z$ , and  $C_0$  [ $\mu\text{mol m}^{-3}$ ] is the atmospheric CO<sub>2</sub> mole density ( $C_0 = 18741.63 \mu\text{mol m}^{-3}$  or 420 ppm). The reference value of 420 ppm was based on the average atmospheric CO<sub>2</sub> concentrations measured by a LI-COR gas analyzer between 16/05-18/06 and 2/7-13/8/2023.  $F_{GM}$  in this study was calculated using CO<sub>2</sub> concentration gradients between 0 and 5 cm depth, as recommended by Chamizo et al. (2022).

205 The relative CO<sub>2</sub> diffusion coefficient in the soil ( $D_s/D_a$  where  $D_a$  [ $\text{m}^2 \text{s}^{-1}$ ] is the CO<sub>2</sub> diffusion coefficient in free air) is estimated based on soil air content-dependent models  $M(\varepsilon)$ , with  $\varepsilon$  being the volumetric air-filled porosity:

$$\frac{D_s}{D_a} = M(\varepsilon) \quad [2]$$

$D_a$  needs to be corrected to in-situ environmental conditions (Jones, 2013) using **Eq. S3**. Models used in this study to calculate  $M(\varepsilon)$ , including the most common models, are listed in **Table 2**.

210 **Table 2: Classical soil diffusion coefficient models used for the GM. Porosity ( $\varphi$ ) values were calculated as described in Eq. S4, and equal to 45%.**

Authors	Model	Originally developed for
Buckingham [1904]	$D_s = D_a \varepsilon^2$	Repacked soils
Penman [1940]	$D_s = 0.66 D_a \varepsilon$	Dry porous materials
Millington & Quirk [1961]	$D_s = D_a \frac{\varepsilon^{10/3}}{\varphi^2}$	Different porous materials
Millington [1959]	$D_s = D_a \varepsilon^{4/3}$	Comparison of published results
Campell [1985]	$D_s = 0.9 D_a \varepsilon^{2.3}$	Aggregated silt loam
Moldrup [2000]	$D_s = D_a \frac{\varepsilon^{2.5}}{\varphi}$	Unstructured natural soils
Marshall [1959]	$D_s = D_a \varepsilon^{1.5}$	Different porous materials
Currie [1970]	$D_s = D_a \left(\frac{\varepsilon}{\varphi}\right)^4 \varphi^{1.5}$	Sand
Lai [1976]	$D_s = D_a \varepsilon^{5/3}$	Undisturbed and repacked soils



Sadeghi [1989]	$D_s = 0.18D_a\left(\frac{\varepsilon}{\phi}\right)^{2.98}$	Soils with clay content from 10.3 to 51.1 %
----------------	---	---

## 2.5. Validation of $F_{GM}$ using $F_{CM}$

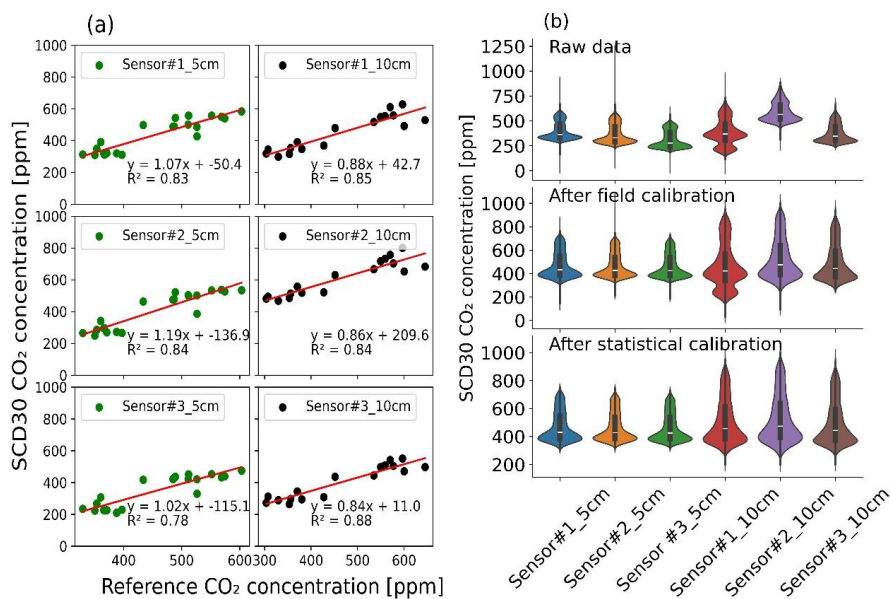
$F_{GM}$  values calculated using the gas diffusion models in **Table. 2** were validated using measured  $F_{CM}$ .  
215 First, we conducted a cross-correlation analysis (Horvatic et al., 2011) between  $F_{CM}$  and  $F_{GM}$  to systematically assess the lag time between measured  $F_{CM}$  and calculated  $F_{GM}$ , which reflects the time delay associated with gas transport from the 5 cm depth to the soil surface as previously reported (Sánchez-Cañete et al., 2017). Then, we shifted the  $F_{GM}$  using the identified lag time to align with the temporal dynamics of  $F_{CM}$ .

## 220 3. Results and discussion

Because this study focuses on the development and field performance of the LC-SS for measuring soil CO<sub>2</sub> concentrations and calculating  $F_{GM}$ , our results and discussion will focus mainly on the LC-SS capabilities, such as long-term stability and accuracy.

### 3.1. CO<sub>2</sub> sensors calibration

225 The field calibration curves for the six low-cost CO<sub>2</sub> sensors are presented in **Fig. 3a**. All sensors show good linearity with high  $R^2 > 0.8$ . The statistical calibration algorithms (**Fig. 2**) improved both the sudden and permanent drifts (**Fig. 3b**). At 5 cm, only 6.6, 2.1, and 4.4 % out of 25,200 readings of sensors #1, #2, and #3, respectively, required correction. At 10 cm, 34.5, 1.9, and 1.39 % readings were corrected for sensor #1, #2, and #3, respectively. The results validate the high stability of the CO<sub>2</sub> sensors after ~6  
230 months. The one exception was sensor#1\_10cm, which exhibited significant data requiring correction. However, the observed drift was systematic; therefore, it was easily corrected by referencing the data from the other two sensors at the same depth (i.e., **Fig. 3b**).



235 **Figure 3: Calibration curves of the SCD30 CO<sub>2</sub> sensors (a) and distribution of CO<sub>2</sub> concentrations collected by six SCD30 CO<sub>2</sub> sensors after each calibration step (b).**

### 3.2. Soil CO<sub>2</sub> concentrations

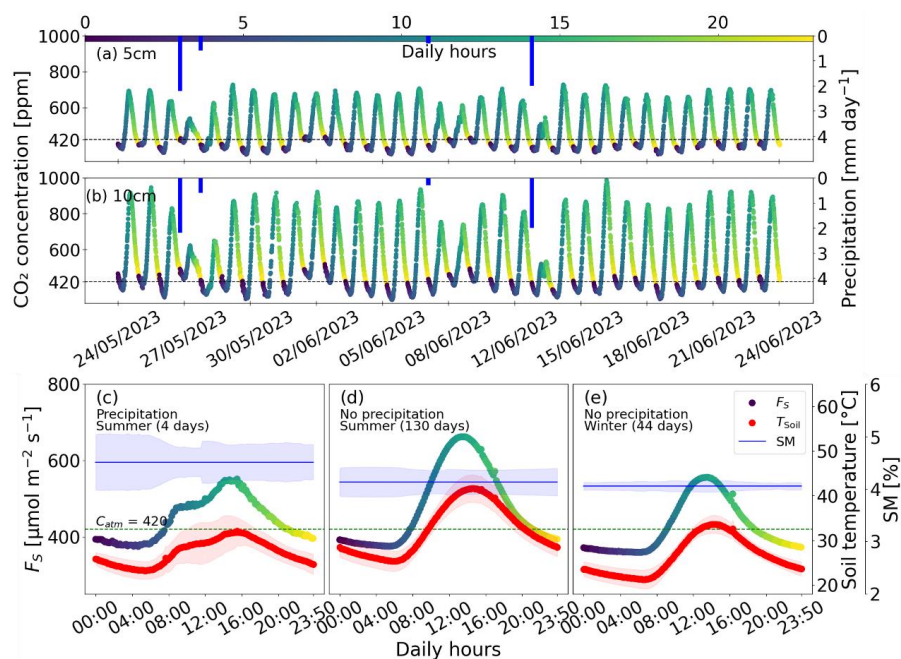
240 The 10-min interval time series of CO<sub>2</sub> concentrations at 5 and 10 cm, and precipitation for one month (24/05-24/06/2023) as an example are shown in **Fig. 4a-b**. The complete dataset for the entire studied period is reported in the supplementary material (**Fig. S2** and **Fig. S3**). The magnitude of CO<sub>2</sub> concentrations at 10 cm was greater than at 5 cm (~340 – ~730 ppm compared to ~320 – ~1000 ppm, respectively). CO<sub>2</sub> concentrations at both depths during daytime (~7:00 – ~21:00 in summer and ~8:00 – ~19:00 in winter) were higher than in the atmosphere, with average daytime concentrations of 545 and 621 ppm at 5 and 10 cm, respectively. However, during nighttime (all hours excluding daytime hours), soil concentrations were lower than in the atmosphere, with average nighttime concentrations of ~380 ppm at both depths. This indicates an efflux of CO<sub>2</sub> from the soil to the atmosphere during daytime in contrast to an influx of CO<sub>2</sub> from the atmosphere into the soil during nighttime. Daytime efflux and nighttime influx were previously observed in arid soils (Cueva et al., 2019; Hamerlynck et al., 2013; Sagi et al., 2021). The study conducted by Sagi et al. (2021) in the Negev Desert revealed a connection between soil CO<sub>2</sub> influx, cooling soil temperatures, and high soil-to-air temperature gradients, specifically occurring when the soil water content (SWC) was below the threshold of ~8%. We observed similar conditions during our study (**Fig. 4c-e**).

250 CO<sub>2</sub> diurnal cycles at 5 cm showed differences between days with and without precipitation (**Fig. 4c-d**) and between summer months (May-September) and winter months (October-November) (**Fig. 4d-e**). On days with precipitation, the average CO<sub>2</sub> concentration increased from 400±20 ppm around 8:00–9:00 to a daily peak of 530±70 ppm at 16:00. On days without precipitation, the morning increase occurred



earlier around 11:00–13:00, reaching  $662 \pm 16$  ppm. Inter-season patterns were also observed, with a winter daily peak lower than the summer daily peak by  $106 \pm 22$  ppm. The occurrence of diurnal cycles during all seasons is a typical phenomenon previously reported (Spohn and Holzheu, 2021; Chamizo et al., 2022).

260 Our results showcase the ability of the underground CO<sub>2</sub> sensor array to capture CO<sub>2</sub> concentration profiles, typical diurnal changes, and seasonal changes. The results also highlight the capability of the sensor array to capture "hot moments", such as the effect of precipitation events on CO<sub>2</sub> concentration in arid soils, significantly contributing to the understanding of the driving mechanisms underlying these moments.



265

**Figure 4:** An example of one month of continuous CO<sub>2</sub> concentration measurements between 24/05-24/06/2023 at 5 cm (a) and 10 cm (b) depths, average daily values at 5 cm of CO<sub>2</sub> concentration, temperature, and soil water content (SWC) during four days with precipitation from May to September (c), 130 days without precipitation between May and September (d), and 44 days without precipitation between October and November (e).

270

### 3.3. F<sub>GM</sub> calculations

The calculated  $F_S$  using the GM ( $F_{GM}$ , Eq. 1) and the measured  $F_S$  using the CM ( $F_{CM}$ ) are presented in Fig. 5a; for simplicity, continuous results from only three representative days without precipitation are shown. Calculated  $F_{GM}$  using different soil gas diffusion models (Table 2) were compared to the  $F_{CM}$ . We observed a time lag in all calculated  $F_{GM}$  compared to the  $F_{CM}$ . Since the  $F_{GM}$  was calculated using the CO<sub>2</sub> concentration gradient between 5 cm and the soil surface,  $F_{GM}$  can only represent subsurface  $F_S$ .

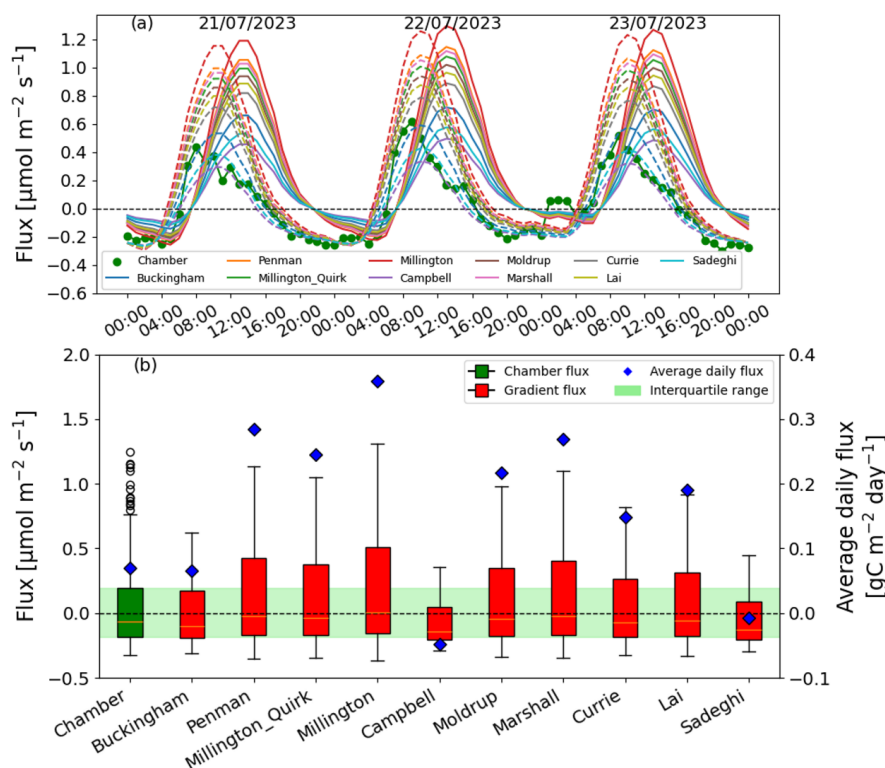
275



Cross-correlation analysis was used to evaluate the lag time between the surface  $F_{CM}$  and the sub-surface  $F_{GM}$ , resulting in a lag time of three hours. To establish temporal alignment between  $F_{GM}$  and  $F_{CM}$ ,  $F_{GM}$  was shifted three hours to the past (**Fig. 5a**, dashed lines).

280 A delay was also observed in the nocturnal influx  $F_{GM}$  compared to the nocturnal influx  $F_{CM}$ . Given the direction of nocturnal  $\text{CO}_2$  exchange—moving from the atmosphere into the soil—at any given moment, the volume of  $\text{CO}_2$  traversing a unit surface area at a given time ( $\text{CO}_2$  influx in units of  $\mu\text{m m}^{-2} \text{s}^{-1}$ ) must exceed that passing through the subsurface region at 5 cm depth. This leads to a more negative nocturnal influx  $F_{CM}$  than nocturnal influx  $F_{GM}$ . Therefore, we used the average daily minimum of nocturnal influx  
285  $F_{CM}$  as a reference to shift the magnitude of  $F_{GM}$ . The time lag between  $F_{GM}$  and  $F_{CM}$  associated with measurement depth was also reported in previous studies (Sánchez-Cañete et al., 2017); the delay generally increases with sensor depth.

The magnitude and distribution of  $F_{CM}$  and  $F_{GM}$  are presented in **Fig. 5b** (box plots). The total net flux over 175 days was calculated by determining the total area under the curve of  $\text{CO}_2$  efflux minus the total  
290 area above the curve of  $\text{CO}_2$  influx. The average daily flux [ $\text{g C m}^{-2} \text{day}^{-1}$ ] was obtained by dividing the total net flux by the total number of days (**Fig. 5b**, blue scatters). Except for the  $F_{GM}$  by the Buckingham gas diffusion model (Buckingham  $F_{GM}$ ), a discrepancy between  $F_{GM}$  and  $F_{CM}$  was observed. Sánchez-Cañete et al., (2017) speculated that *ex-situ* gas diffusion models yield substantial uncertainties when applied to other soils simply because these models were developed based on soil porosity and SWC of  
295 specific soil types (**Table 2**). In comparison to  $F_{CM}$ , Buckingham  $F_{GM}$  was the most comparable, for both magnitude and distribution, as well as average daily net flux. The outliers observed from the boxplot of  $F_{CM}$  correspond to  $\text{CO}_2$  fluxes induced by precipitation events on 28/05/2023, 13/06-2023, and 9/10/2023.



300 **Figure 5: Diurnal cycles of  $F_S$  measured by the chamber method ( $F_{CM}$ , green scatters), by the**  
**gradient method ( $F_{GM}$ , solid lines), and by the gradient method using a 3-hour lag time (dashed**  
**lines) during three representative days without precipitation (a), comparison of  $F_{CM}$  (green) and**  
 **$F_{GM}$  (red; calculated using published gas diffusion models), and average daily flux (blue scatter)**  
**(b).**

305 The linear regression between Buckingham  $F_{GM}$  and measured  $F_{CM}$  is presented in **Fig. 6a** ( $R^2 = 0.70$ ).  
 $F_S$  obtained by these two methods correlated mostly on days without precipitation (**Fig. 6b**). In contrast,  
 on days with precipitation such as 13/06/2023 with  $2 \text{ mm day}^{-1}$ , large variations between the two methods  
 were observed (**Fig. 6c**). The instantaneous increase of  $F_{CM}$  due to precipitation was a well-recognized  
 phenomenon when rewetting occurs in water-limited arid soils (Andrews et al., 2023; Barnard et al.,  
 310 2020; Fierer & Schimel, 2003). The observed  $\text{CO}_2$  pulse, as measured by CM, agrees with the observed  
 pattern of very high rates right after rewetting and slowly declines over time by Kim et al. (2012). These  
 precipitation-induced  $\text{CO}_2$  pulses were underestimated by the GM. Previous studies also reported that  
 the GM did not capture the abrupt  $\text{CO}_2$  pulse increases after water application (Jiang et al., 2022; Yang  
 et al., 2018). Therefore, the utility of the GM in general is often accompanied by a validation/calibration  
 315 using a short-term  $F_S$  measurement for the CM (Chamizo et al., 2022; Sánchez-Cañete et al., 2017).

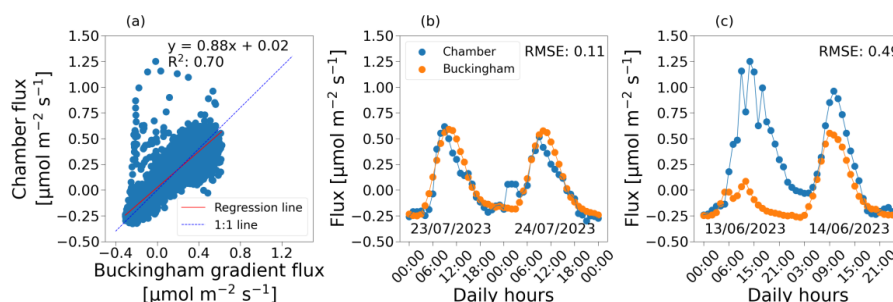


**Figure 6: Linear regression between the Buckingham gradient flux ( $F_{GM}$ ) and the chamber flux ( $F_{CM}$ ) (a), the Buckingham  $F_{GM}$  and the  $F_{CM}$  during two days without precipitation (23-24/07/2023) (b), and during two days with precipitation (13-14/06/2023) (c).**

### 320 3.3. Limitation and modification

We acknowledge that the  $F_{GM}$  calculation method has its limitations.  $F_{GM}$  calculation requires an accurate diffusion coefficient of  $\text{CO}_2$  between 5 cm and the soil surface. This study did not directly measure but used models to estimate the diffusion coefficient, supplemented by  $F_{CM}$  measurements for validation.  $F_{CM}$  measurements, which require chambers and a LI-COR gas analyzer, may pose a cost constraint for resource-limited research. This limitation is not unique to the LC-SS but applies to GM regardless of the sensor type. Even though using  $F_{CM}$  measured by high-end gas analyzers to validate  $F_{GM}$  is a recommended practice (Chamizo et al., 2022; Sánchez-Cañete et al., 2017) and applied in this study, it is not inherently obligatory. An alternative is to measure site-specific diffusion coefficient and calculate  $F_{GM}$  without using published gas diffusion models. For example, Osterholt et al. (2022) suggested an approach to inject  $\text{CO}_2$  as a tracer gas to estimate diffusion coefficient. Furthermore, high-end, expensive chambers and gas analyzers can also be replaced with a low-cost, open-source chamber system (e.g., Forbes et al., 2023). When used with the LC-SS, only one chamber-gas analyzer system per several LC-SSs is needed since only a short duration of  $F_{CM}$  measurements is required for validation.

The LC-SS presented here relies exclusively on an SD card for data logging and storage, which requires manual data retrieval and lacks real-time accessibility for monitoring and troubleshooting. Alternatively, we introduce an updated version of LS-SS equipped with a modem for real-time data updates and immediate troubleshooting whenever necessary (e.g., Levintal., et al., 2021). A detailed, step-by-step, do-it-yourself guide for the updated version is also available on our GitHub page.

## 4. Conclusions

This study introduces an innovative LC-SS developed for continuous, long-term monitoring of soil  $\text{CO}_2$  concentration and  $F_s$ , facilitating in-situ soil-gas-related research. The LC-SS was built from low-cost, readily available hardware and open-source software components. The LC-SS design emphasizes modularity, with publicly available, comprehensive, technical documentation for each module, allowing straightforward replication and customization for non-engineering, low-budget end-users worldwide.





345 The LC-SS was field-tested for ~6 months, showcasing high stability, minimal maintenance  
requirements, and capabilities to capture the temporal dynamics of soil CO<sub>2</sub> concentrations, including  
diurnal and seasonal variabilities. Furthermore, the agreement observed between the calculated  $F_{GM}$  and  
measured  $F_{CM}$ , both in the short term (i.e., sub-daily fluctuation) and in the long term (i.e., net CO<sub>2</sub>  
exchange over ~6 months), demonstrate the potential of the LC-SS as a new approach for  $F_s$   
350 quantification.

In conclusion, the LC-SS, priced at ~USD700, not only provides high accuracy of  $F_s$  but also offers  
higher temporal resolution and the potential for improved spatial resolution if widely adopted. This, in  
turn, could contribute to a more comprehensive dataset for regional-to-global estimation of  $F_s$  and  
advancing our understanding of the global soil carbon cycle.

#### 355 **Data Availability**

The data are available within the above manuscript, the supplementary information, and our GitHub  
repository.

#### **Author Contributions**

TTN and EL conceptualized and conducted the study and wrote the first manuscript draft. EL provided  
360 the resources. All the authors (TTN, NB, AA, MM, NA, and EL) contributed to the final version.

#### **Competing interests**

The authors declare that they have no conflict of interest.

#### **Acknowledgement**

The authors thank Elyasaf Freiman for helping with the field experiments.



365 **References**

- Andrews, H. M., Krichels, A. H., Homyak, P. M., Piper, S., Aronson, E. L., Botthoff, J.,  
Greene, A. C., & Jenerette, G. D. (2023). Wetting-induced soil CO<sub>2</sub> emission pulses are  
driven by interactions among soil temperature, carbon, and nitrogen limitation in the  
Colorado Desert. *Global Change Biology*, 29(11), 3205–3220.  
370 <https://doi.org/10.1111/gcb.16669>
- Barnard, R. L., Blazewicz, S. J., & Firestone, M. K. (2020). Rewetting of soil: Revisiting the  
origin of soil CO<sub>2</sub> emissions. In *Soil Biology and Biochemistry* (Vol. 147). Elsevier Ltd.  
<https://doi.org/10.1016/j.soilbio.2020.107819>
- Bastviken, D., Sundgren, I., Natchimuthu, S., Reyier, H., & Gällfalk, M. (2015). Technical  
375 Note: Cost-efficient approaches to measure carbon dioxide (CO<sub>2</sub>) fluxes and  
concentrations in terrestrial and aquatic environments using mini loggers.  
*Biogeosciences*, 12(12), 3849–3859. <https://doi.org/10.5194/bg-12-3849-2015>
- Bekin, N., & Agam, N. (2023). Rethinking the deployment of static chambers for CO<sub>2</sub> flux  
measurement in dry desert soils. *Biogeosciences*, 20(18), 3791–3802.  
380 <https://doi.org/10.5194/bg-20-3791-2023>
- Blackstock, J. M., Covington, M. D., Perne, M., & Myre, J. M. (2019). Monitoring  
Atmospheric, Soil, and Dissolved CO<sub>2</sub> Using a Low-Cost, Arduino Monitoring  
Platform (CO<sub>2</sub>-LAMP): Theory, Fabrication, and Operation. *Frontiers in Earth Science*,  
7. <https://doi.org/10.3389/feart.2019.00313>
- 385 Bond-Lamberty, B. (2018). New Techniques and Data for Understanding the Global Soil  
Respiration Flux. *Earth's Future*, 6(9), 1176–1180.  
<https://doi.org/10.1029/2018EF000866>
- Bond-Lamberty, B., Ballantyne, A., Berryman, E., Fluet-Chouinard, E., Jian, J., Morris, K.  
A., Rey, A., & Vargas, R. (2024). Twenty Years of Progress, Challenges, and  
390 Opportunities in Measuring and Understanding Soil Respiration. *Journal of Geophysical  
Research: Biogeosciences*, 129(2). <https://doi.org/10.1029/2023JG007637>
- Bond-Lamberty, B., Christianson, D. S., Malhotra, A., Pennington, S. C., Sihi, D.,  
AghaKouchak, A., Anjileli, H., Altaf Arain, M., Armesto, J. J., Ashraf, S., Ataka, M.,  
Baldocchi, D., Andrew Black, T., Buchmann, N., Carbone, M. S., Chang, S. C., Crill, P.,  
395 Curtis, P. S., Davidson, E. A., ... Zou, J. (2020). COSORE: A community database for  
continuous soil respiration and other soil-atmosphere greenhouse gas flux data. *Global  
Change Biology*, 26(12), 7268–7283. <https://doi.org/10.1111/gcb.15353>
- Bond-Lamberty, B., & Thomson, A. (2010). A global database of soil respiration data.  
*Biogeosciences*, 7(6), 1915–1926. <https://doi.org/10.5194/bg-7-1915-2010>
- 400 Bouma, J. (2017). How Alexander Von Humboldt's life story can inspire innovative soil  
research in developing countries. *SOIL*, 3(3), 153–159. <https://doi.org/10.5194/soil-3-153-2017>
- Buckingham, E. (1904), Contributions to Our Knowledge of the Aeration of Soils, U.S. Dept.  
of Agriculture, Bureau of Soils, Washington, D. C.
- 405 Brändle, J., & Kunert, N. (2019). A new automated stem CO<sub>2</sub> efflux chamber based on  
industrial ultra-low-cost sensors. *Tree Physiology*, 39(12), 1975–1983.  
<https://doi.org/10.1093/treephys/tpz104>



- 410 Carbone, M. S., Seyednasrollah, B., Rademacher, T. T., Basler, D., Le Moine, J. M., Beals, S., ... & Richardson, A. D. (2019). Flux Puppy—An open-source software application and portable system design for low-cost manual measurements of CO<sub>2</sub> and H<sub>2</sub>O fluxes. *Agricultural and Forest Meteorology*, 274, 1-6. <https://doi.org/10.1016/j.agrformet.2019.04.012>
- Campbell, G. S. (1985). *Soil physics with BASIC: transport models for soil-plant systems*. Elsevier.
- 415 Chamizo, S., Rodríguez-Caballero, E., Sánchez-Cañete, E. P., Domingo, F., & Cantón, Y. (2022). Temporal dynamics of dryland soil CO<sub>2</sub> efflux using high-frequency measurements: Patterns and dominant drivers among biocrust types, vegetation and bare soil. *Geoderma*, 405. <https://doi.org/10.1016/j.geoderma.2021.115404>
- 420 Chan, K., Schillereff, D. N., Baas, A. C. W., Chadwick, M. A., Main, B., Mulligan, M., O'Shea, F. T., Pearce, R., Smith, T. E. L., van Soesbergen, A., Tebbs, E., & Thompson, J. (2021). Low-cost electronic sensors for environmental research: Pitfalls and opportunities. *Progress in Physical Geography*, 45(3), 305–338. <https://doi.org/10.1177/0309133320956567>
- 425 Cueva, A., Volkmann, T. H. M., van Haren, J., Troch, P. A., & Meredith, L. K. (2019). Reconciling negative soil CO<sub>2</sub> fluxes: Insights from a large-scale experimental hillslope. *Soil Systems*, 3(1), 1–20. <https://doi.org/10.3390/soilsystems3010010>
- Curtis Monger, H., Kraimer, R. A., Khresat, S., Cole, D. R., Wang, X., & Wang, J. (2015). Sequestration of inorganic carbon in soil and groundwater. *Geology*, 43(5), 375–378. <https://doi.org/10.1130/G36449.1>
- 430 Currie, J. A. (1970). Movement of gases in soil respiration. *Sorption and Transport Processes in Soils*, 37(1970), 152-171.
- Davidson, E. A., Savage, K. V. L. V., Verchot, L. V., & Navarro, R. (2002). Minimizing artifacts and biases in chamber-based measurements of soil respiration. *Agricultural and forest meteorology*, 113(1-4), 21-37. [https://doi.org/10.1016/S0168-1923\(02\)00100-4](https://doi.org/10.1016/S0168-1923(02)00100-4)
- 435 De Jong, E., & Schappert, H. J. V. (1972). Calculation of soil respiration and activity from CO<sub>2</sub> profiles in the soil. *Soil Science*, 113(5), 328–333. <https://doi.org/10.1097/00010694-197205000-00006>
- 440 Dennis D. Baldocchi, Bruce B. Hincks, & Tilden P. Meyers. (1988). Measuring Biosphere-Atmosphere Exchanges of Biologically Related Gases with Micrometeorological Methods. *Ecology*, 69(5), 1331–1340. <https://doi.org/10.2307/1941631>
- Fierer, N., & Schimel, J. P. (2003). A Proposed Mechanism for the Pulse in Carbon Dioxide Production Commonly Observed Following the Rapid Rewetting of a Dry Soil. *Soil Science Society of America Journal*, 67(3), 798–805. <https://doi.org/10.2136/sssaj2003.7980>
- 445 Forbes, E., Benenati, V., Frey, S., Hirsch, M., Koech, G., Lewin, G., Mantas, J. N., & Caylor, K. (2023). Fluxbots: A Method for Building, Deploying, Collecting and Analyzing Data From an Array of Inexpensive, Autonomous Soil Carbon Flux Chambers. *Journal of Geophysical Research: Biogeosciences*, 128(6). <https://doi.org/10.1029/2023JG007451>
- 450 Friedlingstein, P., O'sullivan, M., Jones, M. W., Andrew, R. M., Gregor, L., Hauck, J., Le Quéré, C., Luijkx, I. T., Olsen, A., Peters, G. P., Peters, W., Pongratz, J., Schwingshackl, C., Sitch, S., Canadell, J. G., Ciais, P., Jackson, R. B., Alin, S. R.,



- Alkama, R., ... Zheng, B. (2022). Global Carbon Budget 2022. *Earth System Science Data*, 14(11), 4811–4900. <https://doi.org/10.5194/essd-14-4811-2022>
- 455 Gu, L., Massman, W. J., Leuning, R., Pallardy, S. G., Meyers, T., Hanson, P. J., Riggs, J. S., Hosman, K. P., & Yang, B. (2012). The fundamental equation of eddy covariance and its application in flux measurements. *Agricultural and Forest Meteorology*, 152(1), 135–148. <https://doi.org/10.1016/j.agrformet.2011.09.014>
- 460 Hamerlynck, E. P., Scott, R. L., Sánchez-Cañete, E. P., & Barron-Gafford, G. A. (2013). Nocturnal soil CO<sub>2</sub> uptake and its relationship to subsurface soil and ecosystem carbon fluxes in a Chihuahuan Desert shrubland. *Journal of Geophysical Research: Biogeosciences*, 118(4), 1593–1603. <https://doi.org/10.1002/2013JG002495>
- Hassan, S., Mushinski, R. M., Amede, T., Bending, G. D., & Covington, J. A. (2023). Integrated Probe System for Measuring Soil Carbon Dioxide Concentrations. *Sensors*, 23(5). <https://doi.org/10.3390/s23052580>
- 465 Heger, A., Kleinschmidt, V., Gröngroft, A., Kutzbach, L., & Eschenbach, A. (2020). Application of a low-cost NDIR sensor module for continuous measurements of in situ soil CO<sub>2</sub> concentration. *Journal of Plant Nutrition and Soil Science*, 183(5), 557–561. <https://doi.org/10.1002/jpln.201900493>
- 470 Helm, J., Hartmann, H., Göbel, M., Hilman, B., Herrera Ramírez, D., & Muhr, J. (2021). Low-cost chamber design for simultaneous CO<sub>2</sub> and O<sub>2</sub> flux measurements between tree stems and the atmosphere. *Tree Physiology*, 41(9), 1767–1780. <https://doi.org/10.1093/treephys/tpab022>
- 475 Hirano, T., Kim, H., & Tanaka, Y. (2003). Long-term half-hourly measurement of soil CO<sub>2</sub> concentration and soil respiration in a temperate deciduous forest. *Journal of Geophysical Research Atmospheres*, 108(20). <https://doi.org/10.1029/2003JD003766>
- Horvatic, D., Stanley, H. E., & Podobnik, B. (2011). Detrended cross-correlation analysis for non-stationary time series with periodic trends. *EPL*, 94(1). <https://doi.org/10.1209/0295-5075/94/18007>
- 480 Jacoby, W. G. (2000). Loess:: a nonparametric, graphical tool for depicting relationships between variables. *Electoral studies*, 19(4), 577–613. [https://doi.org/10.1016/S0261-3794\(99\)00028-1](https://doi.org/10.1016/S0261-3794(99)00028-1)
- 485 Jian, J., Vargas, R., Anderson-Teixeira, K., Stell, E., Herrmann, V., Horn, M., Kholod, N., Manzon, J., Marchesi, R., Paredes, D., & Bond-Lamberty, B. (2021). A restructured and updated global soil respiration database (SRDB-V5). *Earth System Science Data*, 13(2), 255–267. <https://doi.org/10.5194/essd-13-255-2021>
- Jiang, P., Chen, X., Missik, J. E. C., Gao, Z., Liu, H., & Verbeke, B. A. (2022). Encoding diel hysteresis and the Birch effect in dryland soil respiration models through knowledge-guided deep learning. *Frontiers in Environmental Science*, 10. <https://doi.org/10.3389/fenvs.2022.1035540>
- 490 Jones, H. G. (1992). Plants and microclimate: a quantitative approach to environmental plant physiology. <https://doi.org/10.1017/CBO9780511845727>
- 495 Kim, D. G., Bond-Lamberty, B., Ryu, Y., Seo, B., & Papale, D. (2022). Ideas and perspectives: Enhancing research and monitoring of carbon pools and land-to-atmosphere greenhouse gases exchange in developing countries. *Biogeosciences*, 19(5), 1435–1450. <https://doi.org/10.5194/bg-19-1435-2022>



- Kim, D. G., Vargas, R., Bond-Lamberty, B., & Turetsky, M. R. (2012). Effects of soil rewetting and thawing on soil gas fluxes: A review of current literature and suggestions for future research. *Biogeosciences*, 9(7), 2459–2483. <https://doi.org/10.5194/bg-9-2459-2012>
- 500 Lal, R. (2005). *Soil Carbon Sequestration Impacts on Global Climate Change and Food Security*. <https://doi.org/10.1126/science.1097396>
- Lai, S.-H., J. M. Tiedje, and A. E. Erickson (1976), In situ measurement of gas diffusion coefficient in soils. *Soil Science Society of America Journal*, 40(1), 3-6. <https://doi.org/10.2136/sssaj1976.03615995004000010006x>
- 505 Levintal, E., Kang, K. L., Larson, L., Winkelman, E., Nackley, L., Weisbrod, N., Selker, J. S., & Udell, C. J. (2021). eGreenhouse: Robotically positioned, low-cost, open-source CO<sub>2</sub> analyzer and sensor device for greenhouse applications. *HardwareX*, e00193. <https://doi.org/10.5281/zenodo.4113959>
- 510 Levintal, E., Suvočarev, K., Taylor, G., & E. Dahlke, H. (2021). Embrace open-source sensors for local climate studies. *Nature*, 599(7883), 32–32. <https://doi.org/10.1038/d41586-021-02981-x>
- Lundegårdh, H. (1927). Carbon Dioxide Evolution of Soil and Crop Growth. *Soil Science*, 23(6), 417–453. <https://doi.org/10.1097/00010694-192706000-00001>
- 515 Maier, M., & Schack-Kirchner, H. (2014). Using the gradient method to determine soil gas flux: A review. *Agricultural and forest meteorology*, 192, 78-95. <https://doi.org/10.1016/j.agrformet.2014.03.006>
- Massman, W. J., & Lee, X. (2002). Eddy covariance flux corrections and uncertainties in long-term studies of carbon and energy exchanges. *Agricultural and Forest Meteorology*, 113(1-4), 121-144. [https://doi.org/10.1016/S0168-1923\(02\)00105-3](https://doi.org/10.1016/S0168-1923(02)00105-3)
- 520 Marshall, T. J. (1959). The diffusion of gases through porous media. *Journal of Soil Science*, 10(1), 79-82. <https://doi.org/10.1111/j.1365-2389.1959.tb00667.x>
- Millington, R. J. (1959). Gas diffusion in porous media. *Science*, 130(3367), 100-102. <https://doi.org/10.1126/science.130.3367.100.b>
- 525 Millington, R. J., & Quirk, J. P. (1961). Permeability of porous solids. *Transactions of the Faraday Society*, 57, 1200-1207. <https://doi.org/10.1039/TF9615701200>
- Moldrup, P., Olesen, T., Gamst, J., Schjønning, P., Yamaguchi, T., & Rolston, D. E. (2000). Predicting the gas diffusion coefficient in repacked soil water-induced linear reduction model. *Soil Science Society of America Journal*, 64(5), 1588-1594. <https://doi.org/10.2136/sssaj2000.6451588x>
- 530 Oertel, C., Matschullat, J., Zurba, K., Zimmermann, F., & Erasmi, S. (2016). Greenhouse gas emissions from soils—A review. *Geochemistry*, 76(3), 327-352. <https://doi.org/10.1016/j.chemer.2016.04.002>
- 535 Osterholt, L., Kolbe, S., & Maier, M. (2022). A differential CO<sub>2</sub> profile probe approach for field measurements of soil gas transport and soil respiration. *Journal of Plant Nutrition and Soil Science*, 185(2), 282–296. <https://doi.org/10.1002/jpln.202100155>
- Penman, H. L. (1940), Gas and vapour movements in the soil: I. The diffusion of vapours through porous solids, *J. Agric. Sci.*, 30, 437–462.



- 540 Sadeghi, A. M., Kissel, D. E., & Cabrera, M. L. (1989). Estimating molecular diffusion coefficients of urea in unsaturated soil. *Soil Science Society of America Journal*, 53(1), 15–18. <https://doi.org/10.2136/sssaj1989.03615995005300010003x>
- Sagi, N., Zaguri, M., & Hawlena, D. (2021). Soil CO<sub>2</sub> influx in drylands: A conceptual framework and empirical examination. *Soil Biology and Biochemistry*, 156. <https://doi.org/10.1016/j.soilbio.2021.108209>
- 545 Sánchez-Cañete, E. P., Scott, R. L., van Haren, J., & Barron-Gafford, G. A. (2017). Improving the accuracy of the gradient method for determining soil carbon dioxide efflux. *Journal of Geophysical Research: Biogeosciences*, 122(1), 50–64. <https://doi.org/10.1002/2016JG003530>
- 550 Stell, E., Warner, D., Jian, J., Bond-Lamberty, B., & Vargas, R. (2021). Spatial biases of information influence global estimates of soil respiration: How can we improve global predictions? *Global Change Biology*, 27(16), 3923–3938. <https://doi.org/10.1111/gcb.15666>
- Tang, J., Baldocchi, D. D., Qi, Y., & Xu, L. (2003). Assessing soil CO<sub>2</sub> efflux using continuous measurements of CO<sub>2</sub> profiles in soils with small solid-state sensors. *Agricultural and Forest Meteorology*, 118(3–4), 207–220. [https://doi.org/10.1016/S0168-1923\(03\)00112-6](https://doi.org/10.1016/S0168-1923(03)00112-6)
- 555 Vargas, R., Baldocchi, D. D., Allen, M. F., Bahn, M., Black, T. A., Collins, S. L., Yuste, J. C., Hirano, T., Jassal, R. S., Pumpanen, J., & Tang, J. (2010). Looking deeper into the soil: Biophysical controls and seasonal lags of soil CO<sub>2</sub> production and efflux. *Ecological Applications*, 20(6), 1569–1582. <https://doi.org/10.1890/09-0693.1>
- 560 Warner, D. L., Bond-Lamberty, B., Jian, J., Stell, E., & Vargas, R. (2019). Spatial Predictions and Associated Uncertainty of Annual Soil Respiration at the Global Scale. *Global Biogeochemical Cycles*, 33(12), 1733–1745. <https://doi.org/10.1029/2019GB006264>
- 565 Xiao, J., Chen, J., Davis, K. J., & Reichstein, M. (2012). Advances in upscaling of eddy covariance measurements of carbon and water fluxes. *Journal of Geophysical Research: Biogeosciences*, 117(1). <https://doi.org/10.1029/2011JG001889>
- Xu, M., & Shang, H. (2016). Contribution of soil respiration to the global carbon equation. *Journal of plant physiology*, 203, 16–28. <https://doi.org/10.1016/j.jplph.2016.08.007>
- 570 Yang, X., Fan, J., & Jones, S. B. (2018). Effect of Soil Texture on Estimates of Soil-Column Carbon Dioxide Flux Comparing Chamber and Gradient Methods. *Vadose Zone Journal*, 17(1), 1–9. <https://doi.org/10.2136/vzj2018.05.0112>